Discharge rate consistency of each channel for UAV-based pneumatic granular fertilizer spreader

Xunwei Wang[1,2,3,4], Rui Jiang[1,2,3,4], Zhiyan Zhou[1,2,3,4*], Cancan Song[5], Xiwen Luo[1,2,3,4], Ruifeng Bao[1,2,3,4], Zichen Lyu[1,2,3,4], Junhao Huang[1,2,3,4], Jianqin Lin[1,2,3,4]

(1. *College of Engineering, South China Agricultural University and Guangdong Laboratory for Lingnan Modern Agriculture, Guangzhou 510642, China*;
2. *Guangdong Provincial Key Laboratory of Agricultural Artificial Intelligence (GDKL-AAI), Guangzhou 510642, China*;
3. *Guangdong Engineering Research Center for Agricultural Aviation Application (ERCAAA), Guangzhou 510642, China*;
4. *Key Laboratory of Key Technology on Agricultural Machine and Equipment (South China Agricultural University), Ministry of Education, Guangzhou 510642, China*;
5. *College of Agricultural Engineering and Food Science, Shandong University of Technology, Zibo 255000, China*)

Abstract: Unmanned aerial vehicles (UAVs) are widely being used to spread granular fertilizer in China. Granular fertilizer spreaders equipped with UAVs are mainly centrifugal disc-type and pneumatic. The multichannel pneumatic granular fertilizer spreaders (MPGFSs) have a banded fertilizer deposition distribution pattern, which are more suitable for variable rate fertilization with high precision requirement than the circular deposition distribution pattern of disc-type granular fertilizer spreaders (DGFSs). However, the existing MPGFS has the disadvantage of inconsistent discharge rate of each channel, which affects the uniformity of fertilization. In order to explore the causes of inconsistent discharge rate of each channel, the discrete element method (DEM) and bench test were performed to analysis the discharge process of the fluted roller fertilizing apparatus and distribution of fertilizer in axial direction of fluted roller. The computational fluid dynamics (CFD) was used to simulate the airflow field of pneumatic system to analyze the influence of airflow on the movement of fertilizer particles. The simulation results of the discharge process of the fluted roller fertilizing apparatus showed that the filling velocity at the axial ends of the fluted roller fertilizing apparatus was lower than that of the middle. The reason was that the filling capacity was weak near the wall. The simulated results of the airflow field without partitions showed that the airflow provided by the axial flow fan was rotational, and this caused the particles to move irregularly in the throat, resulting in inconsistency discharge rate of each channel. Based on the analysis of reasons of inconsistent discharge rate of each channel, a MPGFS with partitions in the throat was developed. The discharge rate bench tests were carried out to optimize the partition spacing parameters, and fertilization test was performed to test the performance of the improved MPGFS. The discharge rate test results showed better consistency with partition. The coefficient of variation (CV) of the discharge rate of each channel was 20.16% without the partition and 7.70% with the optimal partition. The fertilizer spreading uniformity bench test results shown that the CV of spreading uniformity of MPGFS without partitions was 15.32%, and that MPGFS with partitions was 8.69%. The partitions design was beneficial to improve the consistency of each channel discharge rate and the uniformity of fertilization. The finding can provide a strong reference to design the MPGFS.

Keywords: UAV, discharge rate, fertilizer spreader, DEM, CFD
DOI: 10.25165/j.ijabe.20231604.7129

Citation: Wang X W, Jiang R, Zhou Z Y, Song C C, Luo X W, Bao R F, et al. Discharge rate consistency of each channel for UAV-based pneumatic granular fertilizer spreader. Int J Agric & Biol Eng, 2023; 16(4): 20–28.

1 Introduction

Fertilization can increase crop yield, but large labor input is needed in production[1]. Traditionally, fertilizer applicators primarily include tractor-based sowing and fertilizing machine and high clearance topdressing machine[2-4]. These heavy ground fertilizer machines are easy to trap in deep paddy fields, easy to crush the ridge, and difficult to transfer. There is also a loss of machine crush when topdressing tall crops. Unmanned aerial vehicles (UAVs) are small in size, has an autonomous obstacle avoidance function, can fly autonomously after planning the route, and are operationally flexible[5]. UAVs can take off and land vertically, fly at low altitudes, and are not restricted by terrain[6], which solves the problem that heavy ground machines are difficult to enter small fields in hilly and mountainous areas. Recently, the application of UAVs in agriculture have undergone rapid development and have been gradually commercialized globally[7,8]. With the enhancement of battery capacity and payload, the application of agricultural

Received date: 2021-10-16 **Accepted date:** 2023-03-11
Biographies: Xunwei Wang, PhD, research interest: agricultural machinery and equipment design, Email: 20201009007@stu.scau.edu.cn; **Rui Jiang**, PhD, Professor, research interest: agricultural aviation application, Email: ruiojiang@scau.edu.cn; **Cancan Song**, PhD, research interest: agricultural machinery and equipment design, Email: 737448145@qq.com; **Xiwen Luo**, PhD, Professor, research interest: rice direct seeding technology and equipment, unmanned farm related technology and intelligent equipment, Email: xwluo@scau.edu.cn; **Ruifeng Bao**, MS candidate, research interest: agricultural machinery and equipment design, Email: 792084698@qq.com; **Zichen Lyu**, MS candidate, research interest: agricultural aviation application, Email: 719269025@qq.com; **Junhao Huang**, MS candidate, research interest: agricultural aviation application, Email: boulet@stu.scau.edu.cn; **Jianqin Lin**, MS candidate, research interest: agricultural aviation application, Email: 602015148@stu.scau.edu.cn.
***Corresponding author: Zhiyan Zhou**, PhD, Professor, research interest: agricultural aviation application, South China Agricultural University, Guangzhou 510642, China, Tel: +86-13560026139, Email: zyzhou@scau.edu.cn.

UAVs has extended to spreading granular fertilizer. Development of fertilizer spreader suitable for UAV has broad application prospects[9].

Many scholars have also conducted research on UAV spreading technology. A rice seed spreader suitable for UAVs has been designed[10]. The device uses a reverse pyramid-shape seed hopper to discharge seeds by self-gravity, and a centrifugal disc to spread seeds. The important parameter of the outlet opening and the disc rotation speed were optimized. The field tests proved it is feasible to spread rice with UAV. Wu et al.[11] designed and optimized a disc-type rice seed spreader with a baffle ring for UAV. Rice seeds ejected by rotating disc are caused to rebound by a baffle ring, to produce a non-hollow, fan-shaped distribution at field level. The discrete element method (DEM) was used to explore the influences of the disc rotation speed, UAV flying height and the angle of the baffle ring. Ren et al.[12] designed a disc-type granular fertilizer spreader (DGFS) for UAV, and optimized the parameters, such as the disc rotation speed and the feeding position angle. Field tests showed that the efficiency of UAV fertilization was 12.5 times that of artificial fertilization, and verified the unique advantages of UAV fertilization on rice topdressing.

In the 1960s, the heavy manned aircraft with multichannel pneumatic granular fertilizer spreader (MPGFS) were used to fertilize large-areas in America[13]. A fluted roller fertilizing apparatus was installed on the abdomen of an aircraft to control the discharge rate of fertilizer, and a pneumatic conveying system was mounted under the fluted roller fertilizing apparatus. Ram-air enters the pneumatic conveying system from the forward of the aircraft, and blows fertilizer backwards. In addition, the pneumatic conveying system was equipped with a diversion channel to distribute the fertilizer to diffuse. Liu et al.[14] optimized the shape and layout of the diversion channel for MPGFS. Bansal et al.[15-17] used computational fluid dynamics (CFD) to study the airflow velocity inside the MPGFS, and coupled with AGDISP (droplet drift simulation software) to study the motion trajectory and velocity of fertilize particles with different diameters. Song et al.[18-20] optimized the MPGFS suitable for UAVs, and designed the variable fertilization system based on prescription map.

The two main types of fertilizer spreader introduced above have their own advantages and disadvantages. Fulton et al.[21] compared and analyzed DGFS and MPGFS. Compared with MPGFS, the DGFS had the advantage of a large discharge rate, but the uniformity of the MPGFS was better. Song et al.[22] comprehensively analyzed the particle distribution uniformity, discharge rate adjustment range, working width, and automatic controllability of two disc-type and two pneumatic fertilization UAVs by analytic hierarchy process method. The analysis demonstrated that the MPGFS has better comprehensive performance. In addition, the MPGFS has a banded fertilizer deposition distribution pattern, which is more suitable for variable rate fertilization than the circular deposition distribution pattern of DGFS.

The research from Song et al.[19,20] focused on the discharge rate control of variable rate fertilization and the adaptability of MPGFS and UAV. The research on the discharge rate consistency of each channel for MPGFS has not been reported. Aiming at the problem of spreading nonuniformity caused by inconsistent discharge rate of each channel, this work will analyze the cause and optimize the structural of the MPGFS. The influence of the airflow field on the discharge rate of each channel was investigated by the CFD simulation. On the basis of exploring the causes for the discharge rate inconsistent of each channel, a MPGFS with partitions in the throat was developed. The distribution pattern of fertilizer falling from the fluted roller fertilizing apparatus along the axial of fluted roller will be researched via DEM simulation, and the axial distribution pattern of fertilizer was used as the basis for the design of the partitions spacing. Finally, the optimized MPGFS will be tested for discharge rate and fertilizer spread uniformity to verify the benefits of improvement. It is expected to improve the performance of MPGFS.

2 Materials and methods

2.1 Structure and working principle of the MPGFS

This fertilizer spreader was designed for UAV. It has the characteristics of light weight, simple disassembly and compact structure. The MPGFS weighed 3.51 kg. The MPGFS consisted of a fluted roller fertilizing apparatus and a pneumatic conveying system with multichannel (Figure 1). The airflow in pneumatic conveying system was supplied by ducted fans. pneumatic conveying system can be divided into an airflow entry section, a throat with material inlet, and a diversion channel. The discharge rate was controlled by adjusting the rotation speed of the fluted roller driven by the stepping motor. When working, the fertilizer flow was discharged from the fluted roller fertilizing apparatus into the throat. Fertilizer was blown in different directions under the combined action of high-speed airflow and diversion channel. Then, a banded fertilizer deposition distribution area was generated along the forward direction of UAV-based MPGFS.

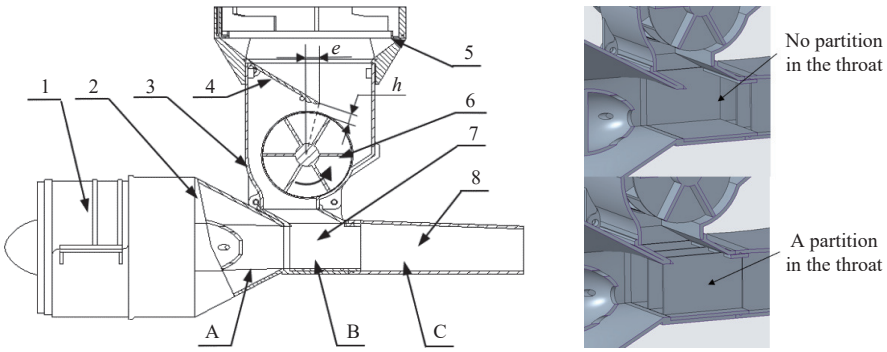

a. Diagram of overall structure of pneumatic broadcaster b. Comparison picture with or without partitions

1.Ducted fan 2.Pneumatic conveying system 3.Fluted roller fertilizing apparatus shell 4.Baffle for removing fertilizer 5.Hopper connector 6.Fluted roller 7.Partitions 8.Diversion channel A.Entry section B.Throat C.Diversion section *e*.Offset of clear fertilizer board *h*. Anticlogging gap

Figure 1 Schematic diagram of the MPGFS

Large and accurate discharge rate is the characteristics of the fluted roller fertilizing apparatus[23,24], which is suitable for variable rate fertilization in precision agriculture[1,25]. The fluted roller fertilizing apparatus was an upper row fluted roller fertilizer discharging device. It was composed of a stepping motor, a fluted roller, a baffle for removing fertilizer, a shell, and other components. To avoid discharge rate pulsation due to sudden releases of fertilizer batches[23], the five rows of staggered fluted roller was used. To prevent clogging, there was an anticlogging gap between the fluted roller and the baffle. To ensure the smooth passage of fertilizer particles, the minimum anticlogging gap was designed to be 5 mm based on fertilizer particle size. The natural angle of repose of the compound fertilizer used in the experiment was measured to be 22.68°. With reference to the design method of the seed-limiting plate[26], the critical value of the offset of the clear fertilizer board was calculated to be 9.09 mm. To prevent the fertilizer from leaking out when the fluted roller was stationary, the offset of the cleaning plate had to be greater than the critical value, rounded to the nearest 10 mm.

There were four vanes with circular arcs in the diversion channel. They were arranged symmetrically, dividing the airflow and fertilizer into five channels (Figure 2). From the top view, the channels were named channels 1-5 from the left to the right. The angle between the outlet direction of channel 1 and the lateral direction was 30°, and the angle between the outlet direction of channel 2 and the lateral direction was 60°.

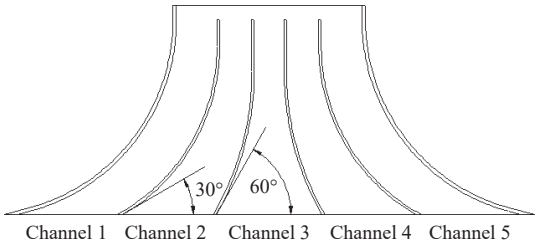

Figure 2 Schematic diagram of the diversion channel

To solve the problem of discharge rate inconsistent of each channel and spreading nonuniformity, the partitions in the throat was developed, as shown in Figure 1b. The partitions were connected with the vans in the diversion channel. The partitions were designed to distribute fertilizer to each channel and to reduce the disordered movement of fertilizer in the throat affected by rotating airflow.

2.2 Causes analysis method of inconsistent discharge rate of each channel

Based on the working principle, fertilizer particle motion is affected by the airflow field in the throat so that the quantity of the fertilizer distributed to each channel is different. Therefore, the mechanism of the airflow field on the distribution of fertilizer particles to channels needs to be studied and to find out the causes for the inconsistency of discharge rate of each channel. The CFD simulation method was used to analyze the airflow field.

The meshing module of ANSYS 19.0 software (ANSYS, Inc., Pennsylvania, USA) was used to mesh the pneumatic conveying system model and the Fluent module to simulate the airflow field. Dynamic mesh method was used to simulate the ducted fans[27]. The model was divided into two parts: the dynamic mesh fluid domain and the static mesh fluid domain. The rotational speed of the dynamic mesh fluid domain was 15 000 r/min. The turbulence model used in the calculation followed the k-ε model[28,29]. The simple algorithm has been adopted, which promotes convergence in the computation of complex flows, to solve the coupling of the velocity and the pressure field[30]. The air inlet of the ducted fan and material inlet of the throat were connected to the atmosphere and established the pressure inlet with a value of 0 Pa. The outlets of the five channels were also connected with the atmosphere and established as the pressure outlet with a value of 0 Pa. The other surfaces were established as walls.

2.3 Design of partitions spacing

The partitions were designed to distribute fertilizer falling from the fluted roller fertilizing apparatus to each channel. In order to distribute the equivalent fertilizer to each channel, the distribution of fertilizer along axial of the groove wheel needs to be clarified when the fertilizer was discharged from the groove wheel fertilizing apparatus. The axial distribution pattern of fertilizer was used as the basis for the design of the partitions spacing. Therefore, the discharging process of the fluted roller fertilizing apparatus was simulated to study the mechanism and axial distribution pattern of the particles using DEM.

2.3.1 DEM model establishment

A three-dimensional model of the fluted roller fertilizing apparatus was created, and it was imported into the EDEM software (DEM Solution Ltd., Edinburgh, UK). A particle factory was established inside the hopper. A particle collection box was established at the fluted roller fertilizing apparatus outlet. The separation planes were established in the collection box, that divided the axial length of the fluted roller fertilizing apparatus outlet into 10 equal parts (Figure 3).

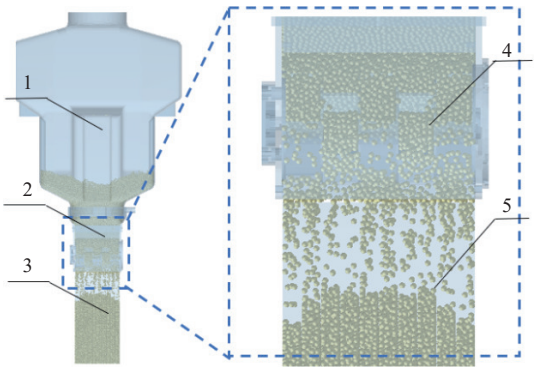

1. Hopper; 2. Fluted roller fertilizing apparatus; 3. Collection box; 4. Fluted roller; 5. Separation plane

Figure 3 EDEM simulation model diagram

To test the applicability of the MPGFS for basal fertilizer application, the compound fertilizer (Guizhou Nuoweishi Biological Engineering Co., Ltd., Guizhou, China) was selected as the research object, and the fertilizer particles were approximately spherical. Randomly selected 200 fertilizers were measured the equivalent diameter to analyze and drew a histogram of the distribution (Figure 4). The normal distribution function of Equation (1) was used to fit the measured data.

$$y = y_0 + Ae^{-\frac{(x-\mu)^2}{2w^2}} \quad (1)$$

where, y is the dependent variable; x is the independent variable; and y_0, A, μ, and w are the coefficients of the normal distribution function. The fitting calculation yielded y_0=0.80, A=25.87, μ=2.96, and w=0.28. The single-sphere model was used as the fertilizer particle model[31,32]. Diameter of fertilizer particle model followed a normal distribution, and the expected value was 2.96 mm.

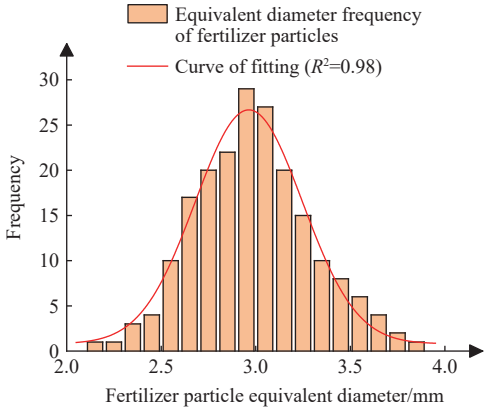

Figure 4 Fertilizer particle equivalent diameter distribution

Table 1 listed the relevant simulation parameters. Because the surfaces of the fertilizer particles were dry and had no adhesion, the Hertz-Mindlin non-slip contact model was applicable. The particle factory generated 150 000 particles in 3 s. The fluted roller began to rotate in the third second, the rotational speed of the fluted roller was 30 r/min, the simulation time step was 1.16×10^{-5} s, and the total simulation time was 10 s.

Table 1 DEM Simulation parameter settings[33]

Parameters	Particles	Models
Poisson's ratio	0.24	0.4
Shear modulus/Pa	1.076×10^{7}	3.266×10^{8}
Density/kg·m^{-3}	1380	1050
Coefficient of restitution with particle	0.27	0.35
Coefficient of rolling friction with particle	0.34	0.32
Coefficient of static friction with particle	0.26	0.47

2.3.2 The bench test method of the axial distribution pattern

To clarify the axial distribution pattern of the fertilizer when the fertilizer particles were discharged from the fluted roller fertilizing apparatus and to verify the correctness of the simulation test, a bench test was conducted. The layout of the test bench is shown in Figure 5a. The rotational speed of the fluted roller was consistent with the simulation test, which was 30 r/min. The fertilizer divider was installed below the outlet of the fluted roller fertilizing apparatus, and the spacing of the partitions was the same as in the simulation model. The fertilizer divider divided the axial length of the fluted roller fertilizing apparatus outlet into 10 equal parts. The fertilizer divider had 10 outlets, connected with collection bottles, numbered 1-10 from left to right. During the test, the fertilizer particles were collected with the collection bottle, and the fertilizer discharge time was 60 s[34]. At the end of each test, the quantity of the fertilizer in each collection bottle were weighted using an electronic scale with an accuracy of 0.1 g.

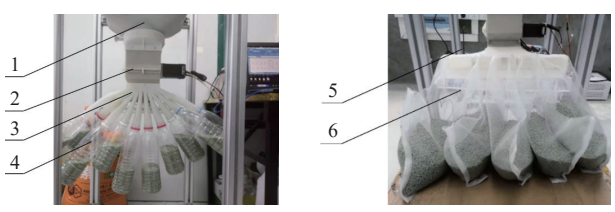

a. Test bench for the particle axial distribution of the fluted roller fertilizing apparatus

b. Test bench for the discharge rate consistency of each channel

1.Hopper 2.Fluted roller fertilizing apparatus 3.Fertilizer divider 4.Collection bottle 5.Diversion channel 6.Collection net bag

Figure 5 Test benches

2.4 The bench test of the discharge rate of each channel

According to the axial distribution law of the particles from the fluted roller fertilizing apparatus, four types of partitions with different spacings were developed, and the spacings were symmetrical (Figure 6). According to the spacing value, they were named center-left 1 (right 1) and left 2 (right 2), respectively. In the example, the first group on the upper left was 17-17-22. The discharge rate consistency test of each channel was conducted on the MPGFS without partitions and with different spacing partitions. The layout of the test bench was shown in Figure 5b. During the test, the rotational speed of the fluted roller was 30 r/min, and the rotational speed of the ducted fan was approximately 15 000 r/min. The net bags were used to collect the fertilizer at each outlet. At the end of each test, the net bag was removed, and the quantity of the fertilizer in each net bag was weighed using an electronic scale.

Figure 6 Partitions with different spacings

To reduce the test error, all of the tests were repeated three times and the average value was taken. For the tests, the index calculation equations are as follows:

$$\overline{x_j} = \frac{1}{n}\sum_{i=1}^{n} x_{ij} \tag{2}$$

$$\overline{x} = \frac{1}{k}\sum_{j=1}^{k} \overline{x_j} \tag{3}$$

$$p_j = \frac{\overline{x_j}}{\overline{x}} \times 100\% \tag{4}$$

$$\sigma = \sqrt{\frac{1}{k-1}\sum_{j=1}^{k} (\overline{x_j} - \overline{x})^2} \tag{5}$$

$$C_v = \frac{\sigma}{\overline{x}} \times 100\% \tag{6}$$

where, $\overline{x_j}$ was the discharge rate of the outlet j of the MPGFS, g/min; x_{ij} was the discharge rate of the outlet j of the MPGFS in the i-th test, g/min; $\overline{x}$ was the average value of the discharge rate of the outlet of the MPGFS, g/min; n was the number of tests; k was the number of the outlets of the MPGFS. p_j was the percentage of the discharge rate (PDR-j) of the outlet j of the MPGFS; σ was the standard deviation of the discharge rate of the outlet of the MPGFS; C_v was the coefficient of variation (CV) of the discharge rate of the outlet of the MPGFS.

2.5 Test method of the spreading uniformity of the MPGFS

The fertilizer spreading uniformity control test was performed in the South China Agricultural University to compare the performance of the MPGFS before and after optimization. In the test, the MPGFS was located on a static bench to obtain the static two-dimensional spread distribution pattern. The indoor operation

can avoid the interference of natural wind and UAV rotor wind, which was helpful to analyze the influence of the MPGFS on the spreading uniformity[35]. The MPGFS and hopper were placed on the elevator and rise to a height of 5 m. A total of 512 collector cartons (0.4 m×0.4 m×0.1 m) were used to cover the 12.8 m×6.4 m spreading area (Figure 7).

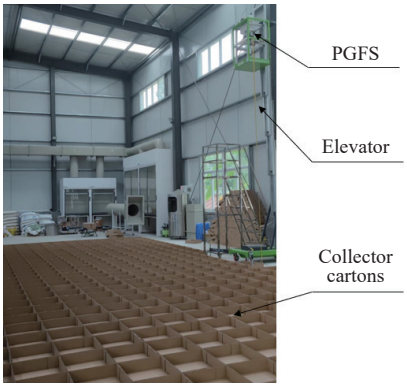

Figure 7 Spreading distribution pattern test bench

Comparative tests of the MGPFS with and without partitions were carried out. The ducted fan rotational speed was approximately 18 000 r/min. The fluted roller rotational speed was 50 r/min. Urea (Henan Xinlianxin Chemicals Group Co., Ltd, Henan, China) with an average particle diameter of 2.98 mm was used. The spreading fertilizer amount was about 1.5 kg. The static spread distribution pattern was got by using an electronic scale with an accuracy of 0.01 g to measure the weight of fertilizer in each collector cartons.

Based on static spreading distribution pattern, The simulation moving spreading distribution pattern was calculated to analyze the spreading uniformity and width by the following steps. 1) The sum of fertilizer amount collected in each column along the simulated moving direction of the MPGFS was divided by the total amount of fertilizer to normalize, and the moving one-dimensional spreading distribution pattern was obtained. 2) The CV of uniformity under different widths was calculated by the method of simulated superposition route[36]. 3) The simulation moving spreading distribution pattern was obtained by using minimum CV as the optimal width. Note that the simulation moving spreading distribution pattern was not the actual deposition, and the results were only used for comparison.

3 Results and analysis

3.1 The causes analysis of inconsistent discharge rate of each channel

3.1.1 Simulation results and analysis of the airflow field without partitions

The simulation results of the pneumatic conveying system without partitions are shown in Figures 8a-8c (the red streamline in Figure 8a indicates that the air velocity was greater than 35 m/s). The outlet air velocity of the ducted fan was greater than 35 m/s, and the airflow was rotational and uneven (Figure 8a). The cross-sectional flow field of the throat after rectification was shown in Figure 8b. The airflow velocity of the throat was approximately 25-27 m/s, but the airflow still rotated. The tangential velocity distribution of the throat is shown in Figure 8c. There were three rotation centers in the airflow field of the throat. The tangential velocity of the airflow in the middle was 11.62 m/s, and the tangential velocity of the airflow on both sides was approximately 5.8 m/s.

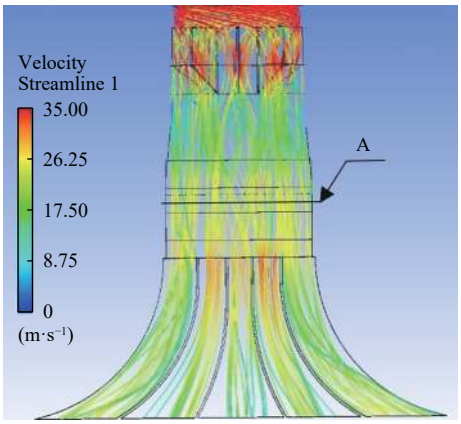

a. Streamline diagram of the airflow field

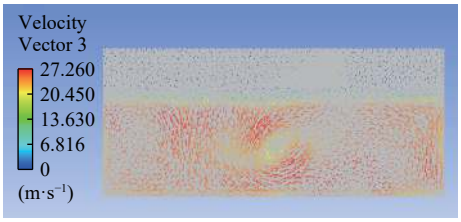

b. Airflow velocity distribution on plane A

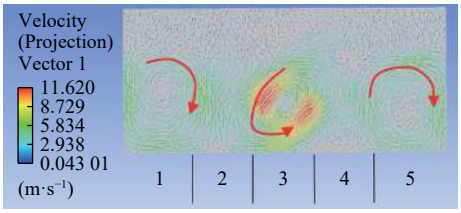

c. Airflow tangential velocity distribution on plane A without partitions

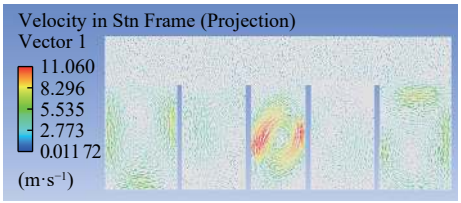

d. Airflow tangential velocity distribution on plane A with the partitions

Figure 8 Simulation results of the airflow field

3.1.2 Simulation results and analysis of the airflow field with partitions

The rotating airflow in the throat will cause the fertilizer particles to motion irregularly, and the discharge rate of the distribution to each channel will be inconsistent. To eliminate the negative influence of the rotating airflow, the partitions were designed in the throat. The partitions can distribute the particles to each channel before they fall into the pneumatic conveying system. The airflow field of the pneumatic conveying system with the partitions was simulated and analyzed, and the tangential velocity distribution of the airflow at the cross-sectional area of the throat is shown in Figure 8d. The airflow in channels 1, 3, and 5 was still rotating. The airflow tangential velocity in channel 3 was 11.06 m/s, and the airflow tangential velocity in channels 1 and 5 were approximately 6.2 m/s. Compared with the pneumatic conveying system without the partitions, it was evident that the partitions could not eliminate the airflow rotation, but could make the airflow rotate only in a single channel without exchange.

3.2 Simulation results and analysis of the fluted roller fertilizing apparatus

To explore the reasons for the axial distribution of fertilizer, the motion law of particles in the fertilizer filling area was investigated using DEM simulation. To observe fertilizer particles motion law in the fertilizer filling area, the particles were manually selected for layering at 3 s, and each layer was marked with a different color, as shown in Figure 9a. At 3.5 s, the position of the particles is shown in Figure 9b. By comparing Figure 9a and Figure 9b, it can be found that the particles on both ends of the fertilizer filling area had poorer fluidity than the particles in the middle.

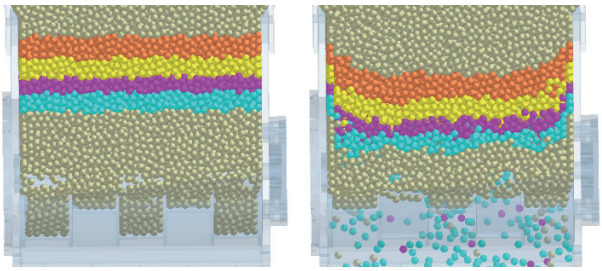

a. 3.0 s b. 3.5 s

Figure 9 Particle mark and position display in the fertilizer filling area

To further study the particles motion law in the fertilizer filling area, the particle velocity was analyzed. The post-processing Grid Bin Group function of EDEM software was utilized to select the 20 mm×5 mm×100 mm grid in the fertilizer filling area (Figure 10). The grid was divided into 10 bins named bin 1-10, and the average magnitude velocity and component velocity of the particles were counted in each bin (Figure 11). The average value of the particle magnitude velocity in the bin 1-10 was 0.0545 m/s. The average value of the particle magnitude velocity in the bin 2-9 was 0.0658 m/s. The *Z* axis velocity was much larger than the *X* and *Y* axis velocity, and the distribution law was consistent with the magnitude velocity. The direction of the *Y* axis velocity was opposite at the two ends of the axis, that was, the particles have an axial velocity from the middle to the two ends. According to the velocity analysis of the particles, the reason of the poor filling capacity on both ends was clarified. In addition, because the particles at both ends fell slowly, a phenomenon occurred in which the particles in the middle moved along the axial direction to supplement the ends.

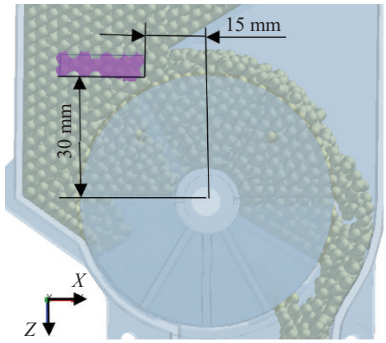

Figure 10 Selection location of the Grid Bin Group

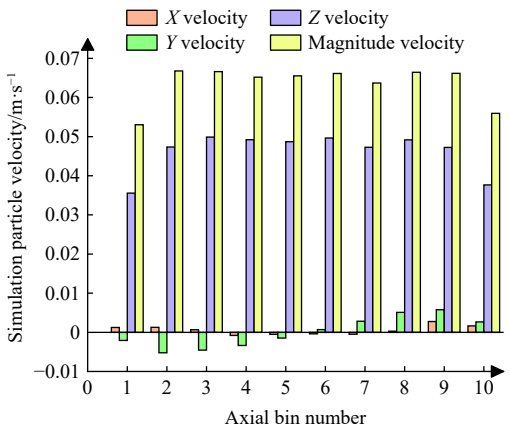

Figure 11 Particle velocity distribution in the fertilizer filling area

3.3 The axial distribution of the fertilizer

To save the simulation running time, the simulation duration was set less than the test duration. This resulted in a large difference in the quantity of discharged particles. To compare the simulation results with the test results and verify the correctness of the simulation results, the particle quantity of each numbered outlet was converted into a PDR-j by Equation (4), and the result is shown in Figure 12. The tested results showed that the PDR-10 was the smallest at 7.96%, PDR-8 was the largest at 10.86%, and the overall CV was 7.42%. The difference between PDR-2 to PDR-9 was small, and the CV was 1.56%. The simulation result showed that the PDR-1 was the smallest, at 9.04%, PDR-5 was the largest at 10.44%, and the overall CV was 5.10%. The error between the simulation and test results was between –4.36% and 13.83%, and the average absolute error was 3.24%. The simulation results were in good agreement with the test results, which demonstrated the correctness of the simulation. The axial distribution of the particles was less on both ends and more in the middle. Therefore, in the discharge rate bench test, four kinds of partitions with small spacing in the middle and large spacing on both sides were designed for test.

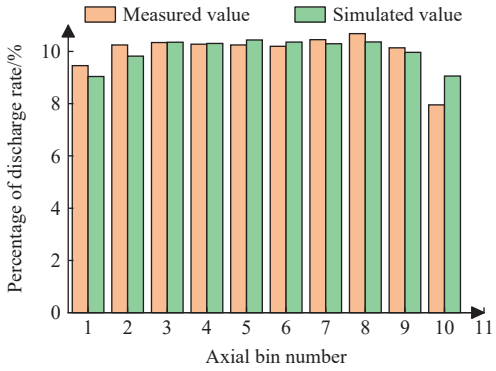

Figure 12 Axial distribution of particles from the fluted roller fertilizing apparatus

3.4 Discharge rate consistency of each channel

The results of the discharge rate consistency of each channel were shown in Figure 13. The channel 2 of the MPGFS with no partitions had the largest discharge rate, accounting for 24.50% of the total discharge rate, and the channel 4 had the smallest discharge rate, accounting for 13.97% of the total discharge rate. The CV of the discharge rate consistency of each channel was 20.16%. Combined with the analysis of the airflow field (Figure 8), it was evident that the tangential velocity of the airflow in the throat was the primary factor that caused the particles to move laterally in the throat. The airflow corresponding to channel 1 rotated clockwise. The airflow corresponding to channel 2 moved downward. The airflow corresponding to channel 3 rotated counterclockwise. Particles fell into the throat from the material inlet, and some particles in the corresponding positions of channels 1 and 3 moved laterally to channel 2 under the action of the tangential velocity of

the airflow. This caused an increase in the particles in channel 2. In addition, there was an upward tangential velocity of the airflow in channel 4 that prevented particles from falling into channel 4, and some particles were laterally distributed to channels 3 and 5, resulting in a decrease of particles in channel 4.

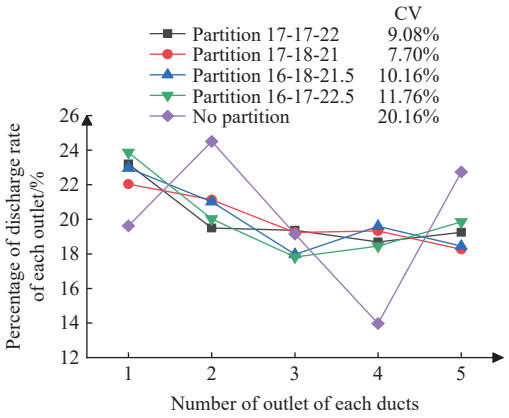

Figure 13 Discharge rate of each outlet under the different partitions

The CV of the discharge rate consistency of each channel of the MPGFS with the partitions was lower than that of the one without the partitions. Among the partitions with different spacing, partitions 17-18-21 were the best, and the CV of the discharge rate consistency of each channel was 7.70%. However, there was a phenomenon of excessive fertilizer on the left side. Since the structure of the MPGFS was symmetrical, it was speculated that this phenomenon was still affected by the rotating airflow.

3.5 The fertilizer spreading uniformity

Figure 14 showed the static spreading distribution patterns of control group and optimized MPGFS. Among them, the partitions were 17-18-21. The results of control group without rectifier showed maximum deposition on the left side with a peak of 12.90 g. At the peak more fertilizer and throat airflow velocity were uneven, resulting in closer blowing distance. The spreading distribution patterns were similar to that of control group with partitions. The peak value on the left side was 12.79 g, and the small peak value on the right side was 9.99 g.

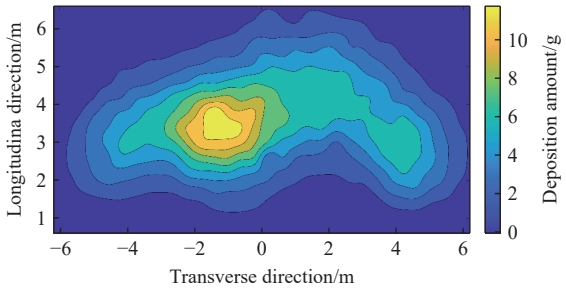

a. No partitions

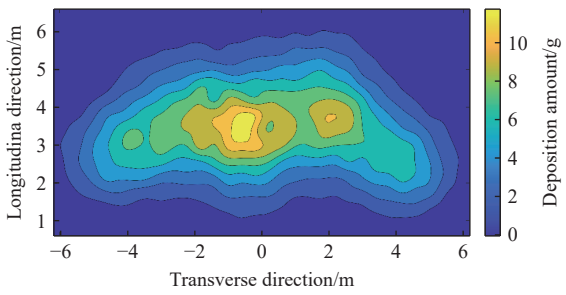

b. With partitions

Figure 14 Static spreading distribution patterns

Figure 15 showed the simulation moving spreading distribution patterns of control group and optimized MPGFS. The results of the control group showed that the minimum uniformity CV was 15.32%, and the available width was 8 m. Minimum uniformity CV was 8.69% and available width was 8.8 m for MPGFS with partitions. There was no simulated superposition route, only from the point of view of moving one-dimensional spreading distribution patterns, there were single peaks in the control group and the partitions, especially in the control group. The asymmetry of both sides of static spreading distribution pattern affects the uniformity of moving spreading distribution pattern of simulated superposition route.

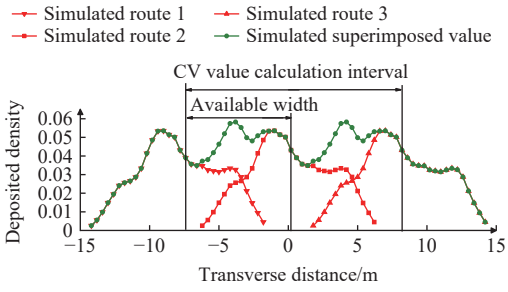

a. No partitions

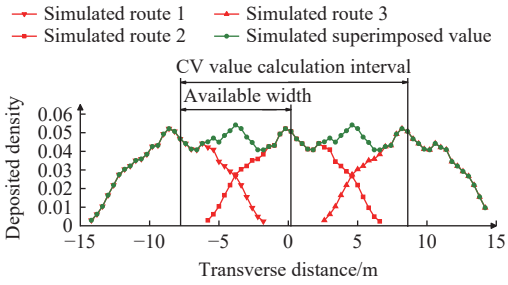

b. With partitions

Figure 15 Simulation moving spreading distribution pattern

4 Discussion

There are many factors contributing to the uniformity results of spreading fertilizer by MPGFS based on UAV, such as the performance of MPGFS, natural winds, rotor winds of UAV, and test methods[37-40]. In this work, from the perspective of improving the performance of the MPGFS, the bench test of MPGFS found that the discharge rate of each channel was inconsistent.

The results have shown that the main reason for the inconsistency of each channel discharge rate was the rotation of the airflow from the duct fan. According to the axial distribution of fertilizer at the outlet of the fluted roller fertilizing apparatus, a reasonable spacing of partitions can effectively improve the discharge rate consistency of each channel. However, the partitions also have disadvantages that the partitions have no rectification effect, rotating airflow still affects the consistency of each channel discharge rate. Grid or honeycomb rectifiers are often designed to rectify airflow in wind tunnels. Further research can be carried out to optimize the performance of the MPGFS and get better results by rectifying the airflow field.

The bench test of fertilizer spreading distribution pattern was carried out indoors, excluding the interference of natural wind and rotor wind, and the distribution pattern of fertilizer could be accurately tested. The distribution pattern of MPGFS without partitions was that the peak was located on the left side, and the

maximum discharge rate of channel 2 in discharge rate test results of each channel can explain this distribution pattern. The fertilizer distribution pattern of the MPGFS with partitions was that the peak value was located in the middle, and the better uniformity can be obtained after the superposition of the two sides of the route. For the triangular distribution pattern with peaks in the middle, the rotation angle of the vans in the diversion channel can be further increased to obtain an ideal trapezoidal distribution pattern. The comparison results before and after optimization showed that the partitions design was beneficial to improve the consistency of each channel discharge rate and the uniformity of fertilization, so this work was meaningful.

5 Conclusions

To improve the performance of the MPGFS, the discharge process of the fluted roller fertilizing apparatus and the airflow field of the pneumatic conveying system were studied via the DEM and CFD simulation. The partitions were developed to improve the discharge rate consistency of each channel, and the following conclusions are drawn:

1) The rotational airflow field was the main cause that affected the consistency of the discharge rate of each channel. The airflow of the pneumatic conveying system was supplied by a ducted fan, so that was rotational in the throat. The simulation results showed that there were three air rotation centers in the throat, among which the tangential velocity of the airflow in the middle approximately 11.62 m/s. The rotation of the airflow caused particles to motion laterally, resulting in uneven distribution of fertilizers to each channel, and the discharge rate consistency of each channel was poor.

2) The discovery of axial distribution pattern has provided a reference for partitions spacing design. Both the test and simulation results showed that the discharge rate of the fluted roller fertilizing apparatus along the axial distribution pattern was less than the middle at both ends. According to the simulation analysis of the particle velocity in the fertilizer filling area, it was concluded that the two ends of the axial were near to the wall surface, resulting in a low particle filling velocity and poor filling ability, and some middle particles were required to fill both ends.

3) Based on axial distribution pattern of fertilizer, four types partitions with different spacings were designed for testing. The results showed that the discharge rate consistency of each channel was the best under the action of partitions 17-18-22, and the consistency CV was 7.70%. The addition of partitions in the throat effectively improved the discharge rate consistency of each channel.

4) The optimized MPGFS was tested for spreading uniformity. The results showed that there was a single peak in the distribution pattern of with or without the partitions. The fertilizer distribution pattern of the MPGFS with partitions was that the peak value was located in the middle, and the better uniformity can be obtained after the superposition of the two sides of the route. According to the analysis of the simulation moving spreading distribution pattern results, the CV of spreading uniformity of MPGFS without partitions was 15.32%, that MPGFS with partitions was 8.69%. The partitions design was beneficial to improve the consistency of each channel discharge rate and the uniformity of fertilization.

Acknowledgements

This work was supported by the Laboratory of Lingnan Modern Agriculture Project (Grant No.NT2021009); the Project of key R&D program of Guangzhou of China (Grant No. 202206010149) , in part by Science and Technology Plan of Jian City of China (Grant No. 20211-055316 and [2020]83), Science and Technology Plan of Guangdong Province of China (2023B10564002 and 2021B 1212040009), Innovative Research Team of Agricultural and Rural Big Data in Guangdong Province of China (2019KJ138). The authors would like to thank the anonymous reviewers for their critical comments and suggestions for improving the manuscript.

[References]

[1] Alameen A A, Al-Gaadi K A, Tola E. Development and performance evaluation of a control system for variable rate granular fertilizer application. Computers and Electronics in Agriculture, 2019; 160: 31–39. doi. org/10.1016/j. compag. 2019.03. 011

[2] Qi X Y, Zhou Z Y, Lin S Y, Xu L. Design of fertilizer spraying device of pneumatic variable-rate fertilizer applicator for rice production. Transactions of the CSAM, 2018; 49(S1): 164–170. (in Chinese)

[3] Shi Y Y, Chen M, Wang X C, Morice O O, Li C G, Ding W M. Design and experiment of variable-rate fertilizer spreader with centrifugal distribution cover for rice paddy surface fertilization. Transactions of the CSAM, 2018; 49(3): 86–93. (in Chinese)

[4] Yang L W, Chen L S, Zhang J Y, Sun H, Liu H J, Li M Z. Test and analysis of uniformity of centrifugal disc spreading. Transactions of the CSAM, 2019; 50(S1): 108–114. (in Chinese)

[5] Zhang C H, Kovacs J M. The application of small unmanned aerial systems for precision agriculture: A review. Precision Agriculture, 2012;13(6): 693–712.

[6] Yang S L, Yang X B, Mo J Y. The application of unmanned aircraft systems to plant protection in China. Precision Agriculture, 2018; 19(2): 278–292. doi. org/10.1007/s11119-017-9516-7.

[7] Zhou Z Y, Ming R, Zang Y, He X G, Luo X W, Lan Y B. Development status and countermeasures of agricultural aviation in China. Transactions of the CSAE, 2017; 33(20): 1–13. (in Chinese)

[8] Hassler S C, Baysal-Gurel F. Unmanned aircraft system (UAS) technology and applications in agriculture. Agronomy, 2019; 9(10): 618.

[9] Wan J J, Qi L J, Zhang H, Lu Z A, Zhou J R. Research status and development trend of UAV broadcast sowing technology in China. An ASABE Meeting Presentation, 2021. doi:org/10.13031/aim.202100017.

[10] Li J Y, Lan Y B, Zhou Z Y, Zeng S, Huang C, Yao W X, et al. Design and test of operation parameters for rice air broadcasting by unmanned aerial vehicle. Int J of Agric &Biol Eng, 2016; 5: 24–32.

[11] Wu Z J, Li M L, Lei X L, Wu Z Y, Jiang C K, Zhou L, et al. Simulation and parameter optimisation of a centrifugal rice seeding spreader for a UAV. Biosystems Engineering, 2020; 192: 275–293. doi:org/10.1016/j.bio systemseng.2020.02.004

[12] Ren W J, Wu Z Y, Li M L, Lei X L, Zhu S L, Chen Y. Design and Experiment of UAV Fertilization Spreader System for Rice. Transactions of the CSAM, 2021; 52(3): 88–98.

[13] Brazelton R W. Dry materials distribution by aircraft. Transactions of the ASAE, 1968; 11(5): 635–641.

[14] Liu C H, Kang Q, Hu S R. Research on model test of aircraft spreader. Transactions of Journal of Jilin University, 1986; 4: 22–30. (in Chinese)

[15] Bansal R K, Walker J T, Gardisser D R. Computer simulation of urea particle acceleration in an aerial spreader. Transactions of the ASAE, 1998; 41(4): 951–957.

[16] Bansal R K, Walker J T, Gardisser D R, Grift T E. Validating FLUENT for the flow of granular materials in aerial spreaders. Transactions of the ASAE, 1998; 41(1): 29–35.

[17] Bansal R K, Walker J T, Gardisser D R. Simulation studies of urea deposition pattern from an aerial spreader. Transactions of the ASAE, 1998; 41(3): 537–544.

[18] Song C C, Zhou Z Y, Zang Y, Zhao L L, Yang W W, Luo X W, et al. Variable-rate control system for UAV-based granular fertilizer spreader. Computers and Electronics in Agriculture, 2021; 180: 105832. doi. org/10.1016/j. compag. 2020.105832.

[19] Song C C, Zhou Z Y, Jiang R, Luo X W, He X G, Ming R. Design and parameter optimization of pneumatic rice sowing device for unmanned aerial vehicle. Transactions of the CSAE, 2018; 34(6): 80–88. (in Chinese)

[20] Song C C, Zhou Z Y, Wang G B, Wang X W, Zang Y. Optimization of the groove wheel structural parameters of UAV-based fertilizer apparatus. Transactions of the CSAE, 2021; 37(22): 1–10. (in Chinese)

[21] Fulton J P, Shearer S A, Higgins S F, Hancock D W, Stombaugh T S. Distribution pattern variability of granular vrt applicators. Transactions of the ASAE, 2005; 48(6): 2053–2064.

[22] Song C C, Zang Y, Zhou Z Y, Luo X W, Zhao L L, Ming R, et al. Test and comprehensive evaluation for the performance of UAV-based fertilizer spreaders. IEEE Access, 2020; 8: 202153–202163.

[23] Sugirbay A M, Zhao J, Nukeshev S O, Chen J. Determination of pin-roller parameters and evaluation of the uniformity of granular fertilizer application metering devices in precision farming. Computers and electronics in agriculture, 2020; 179: 105835. doi:org/10.1016/j.compage. 2020.105835.

[24] Zeng S, Tan Y P, Wang Y, Luo X W, Yao L M, Huang D P, et al. Structural design and parameter determination for fluted-roller fertilizer applicator. Int J Agric & Biol Eng, 2020; 13(2): 101–110.

[25] Sahin M, Habib K. Design and development of an electronic drive and control system for micro-granular fertilizer metering unit. Computers and Electronics in Agriculture, 2019; 162: 921–930. doi. org/10.1016/j. compag. 2019.05. 048.

[26] Zhang M H, Wang Z M, Luo X W, Dai Y Z, He X, Wang B L. Effect of double seed-filling chamber structure of combined type-hole metering device on filling properties. Transactions of the CSAE, 2018; 34(12): 8–15. (in Chinese)

[27] Deng Y P, Mi B G, Zhang Y. Research on numerical calculation for aerodynamic characteristics analysis of ducted fan. Transactions of Journal of Northwestern Polytechnical University, 2018; 36(6): 1045–1051. (in Chinese)

[28] Fernández Oro J M, Pereiras García B, González J, Argüelles Díaz K M, Velarde-Suárez S. Numerical methodology for the assessment of relative and absolute deterministic flow structures in the analysis of impeller–tongue interactions for centrifugal fans. Computers & Fluids, 2013; 86: 310–325. doi. org/10.1016/j. compfluid. 2013.07. 014.

[29] Ye X M, Ding X L, Zhang J K, Li C X. Numerical simulation of pressure pulsation and transient flow field in an axial flow fan. Energy (Oxford), 2017; 129: 185–200. doi. org/10.1016/j. energy. 2017.04. 076.

[30] Li C X, Lin Q, Ding X L, Ye X M. Performance, aeroacoustics and feature extraction of an axial flow fan with abnormal blade angle. Energy (Oxford), 2016; 103: 322–339. doi. org/10.1016/j. energy. 2016.02. 147.

[31] Liu J S, Gao C Q, Nie Y J, Yang B, Ge R Y, Xu Z H. Numerical simulation of Fertilizer Shunt-Plate with uniformity based on EDEM software. Computers and Electronics in Agriculture, 2020; 178: 105737. doi. org/10.1016/j. compag. 2020.105737.

[32] Sun J F, Chen H M, Duan J L, Liu Z, Zhu Q C. Mechanical properties of the grooved-wheel drilling particles under multivariate interaction influenced based on 3D printing and EDEM simulation. Computers and Electronics in Agriculture, 2020; 172: 105329. doi. org/10.1016/j. compag. 2020.105329.

[33] Shi Y Y, Chen M, Wang X C, Morice O O, Ding W M. Numerical simulation of spreading performance and distribution pattern of centrifugal variable-rate fertilizer applicator based on DEM software. Computers and electronics in agriculture, 2018; 144: 249–259. doi. org/10.1016/j. compage. 2017.12. 015.

[34] Gao L P, Chen H, Liao Q X, Zhang Q S, Li Y B, Liao Y T. Experiment on Fertilizing Performance of Dynamic Tilt Condition of Seeder with Deep Fertilizer for Rapeseed. Transactions of the CSAM, 2020; 51(S1): 64–72. (in Chinese)

[35] Coetzee C J, Lombard S G. Discrete element method modelling of a centrifugal fertiliser spreader. Biosystems Engineering, 2011; 109(4): 308–325.

[36] ASAE. Calibration and Distribution Pattern Testing of Agricultural Aerial Application Equipment. ASAE Standard S386.2. 2013., 2013.

[37] Cool S R., Vangeyte J, Mertens K C., Nuyttens D R E, Sonck B R, Gucht T C V D, et al. Comparing different methods of using collecting trays to determine the spatial distribution of fertiliser particles. Biosystems Engineering, 2016; 150: 142-150. doi. org/10.1016/j. biosystemseng. 2016.08. 001.

[38] Zhan Y L, Chen P C, Xu W C, Chen S D, Han Y F, Lan Y B, et al. Influence of the downwash airflow distribution characteristics of a plant protection UAV on spray deposit distribution. Biosystems Engineering, 2022; 216: 32–45. doi. org/10.1016/j. biosystemseng. 2022.01. 016.

[39] Chen S D, Lan Y B, Zhou Z Y, Fan O Y, Wang G B, Huang X Y, et al. Effect of Droplet Size Parameters on Droplet Deposition and Drift of Aerial Spraying by Using Plant Protection UAV. Agronomy, 2020; 10(2): 195.

[40] Cool S R, Pieters J G, Acker J V, Bulcke J V D, Mertens K C, Nuyttens D R E, et al. Determining the effect of wind on the ballistic flight of fertiliser particles. Biosystems Engineering, 2016; 151: 425–434. doi. org/10.1016/j. biosystemseng. 2016.10. 011.